Mono- and Tetra-nuclear Manganese(III) Complexes of Tripodal Tris[2-(salicylideneamino)ethyl]amines†

Swapan Kumar Chandra, Partha Chakraborty and Animesh Chakravorty*
Department of Inorganic Chemistry, Indian Association for the Cultivation of Science, Calcutta 700032, India

The tripodal ligands $N[CH_2CH_2N{=}CHC_6H_3X(OH)\text{-}2]_3$ (X = H, H_3L^1 or Cl-5, H_3L^2] afford the mononuclear complexes [$Mn^{III}L$]. Structural work has shown that the symmetry of the facial MnN_3O_3 co-ordination sphere in the two solvates [MnL^2]·$3H_2O$ and [MnL^2]·MeOH varies considerably as the former has C_3 and the latter C_1 symmetry. The implications of these differences are discussed. Reaction of [MnL] with manganese(III) acetate dihydrate in alkaline media affords the antiferromagnetic tetranuclear cations $[Mn^{III}_4O_2L_2]^{2+}$ in high yields. X-Ray studies on $[Mn_4O_2L^1_2][PF_6]_2$·4MeCN have revealed a centrosymmetric $Mn_4(\mu_3\text{-}O)_2^{8+}$ core, with the shortest Mn···Mn contact being 2.906(3) Å. The metal co-ordination spheres are of two types: facial-MnN_3O_3 and $MnNO_5$. The cyclic voltammograms of $[Mn_4O_2L_2]^{2+}$ display two successive waves due to the Mn^{III}–Mn^{II} couples of the MnN_3O_3 spheres. For [MnL] only one such couple is observed. Oxidative responses due to Mn^{IV}–Mn^{III} couples are also observed. Some preliminary work on an iron(III) analogue of $[Mn_4O_2L_2]^{2+}$ is also described.

The mononuclear binding of 3d metal(III) ions by the tripodal ligand[1] H_3L is known to afford complexes of co-ordination type **I**.[2-5] The ligand also appeared to be potentially well suited to polynuclear binding and this has led us to investigate its transition-metal chemistry. Herein we report two new findings on manganese(III) complexes of H_3L. One is the occurrence of a MnN_3O_3 co-ordination sphere for a mononuclear complex [MnL] in two solid-state forms differing markedly in symmetry and dimensions. The other and more important finding is that H_3L can support polynucleation, as revealed by the facile transformation of [MnL] into the tetranuclear entity $[Mn_4O_2L_2]^{2+}$. The latter has been isolated and characterised in a number of salts. The structure, magnetism, electronic spectra and electroactivity of the tetranuclear species are examined in relation to those of the mononuclear complexes. The feasibility of extending the tetranucleation reaction to the case of iron(III) is also studied briefly. A preliminary communication on the manganese(III) system was published by us some time ago,[6] and several months later a second communication appeared.[7]

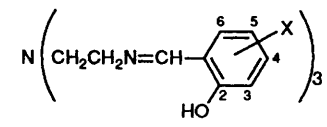

H_3L

X = H H_3L^1
X = Cl-5 H_3L^2

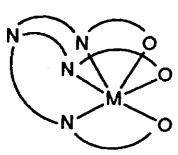

I

Results and Discussion

The two H_3L type ligands used in the present work were H_3L^1 (X = H) and H_3L^2 (X = Cl-5). The green, high-spin[2-4] mononuclear manganese(III) complexes were synthesised by treating manganese(III) acetate dihydrate with H_3L in methanol. Recrystallisation from dichloromethane–methanol (1 : 1) afforded crystals of the methanol adducts [MnL^1]·MeOH and [MnL^2]·MeOH. Hydrated crystals of composition [MnL^2]·$3H_2O$ were obtained from wet acetonitrile, but a similar trihydrate of [MnL^1] did not crystallise under analogous conditions. Crystals of [MnL^2]·$3H_2O$ were obtained previously from wet dimethylformamide.[3]

Structures of [MnL^2]·$3H_2O$ *and* [MnL^2]·MeOH. *Two Forms of the* MnN_3O_3 *Co-ordination Sphere.*—In the cubic crystals (space group $I\bar{4}3$) of the previously characterised [MnL^2]·$3H_2O$, isolated from wet dimethylformamide, the metal atom and the unco-ordinated tripodal nitrogen atom lie on a crystallographic three-fold axis imposing a strict C_3 symmetry on the [MnL^2] molecule.[3] The phenolic oxygens of adjacent molecules (lying on the same C_3 axis) are linked by three pairs of hydrogen-bonded water molecules.[2,3] Since C_3 symmetry for the high-spin d^4 manganese(III) ion is unusual (see below) we therefore determined the structure of our sample of [MnL^2]·$3H_2O$ prepared from wet acetonitrile. Our results[8] fully agree with the previous findings[3] and the details are therefore not reproduced here.

Crystals of [MnL^2]·MeOH belong to the space group $P\bar{1}$ and a view of the molecule is shown in Fig. 1. Selected bond parameters are listed in Table 1. The metal co-ordination sphere is distorted octahedral with strong axial elongation (see below) and the tripodal nitrogen is not co-ordinated. The methanol molecule is not bonded to any atom or group. The structure is generally similar to that[6] of [MnL^1]·MeOH which, however, crystallises in the monoclinic system $P2_1/n$ with the MeOH molecule hydrogen bonded to one of the phenolic oxygen atoms.[9]

The metal–ligand distances and anisotropic thermal behaviour within the co-ordination spheres of the two [MnL^2] solvates are compared in Fig. 2. In [MnL^2]·$3H_2O$, the Mn–N distances are all equal by symmetry as are all the Mn–O distances. In contrast, the Mn–N(4) and Mn–O(1) bonds

† *Supplementary data available:* see Instructions for Authors, *J. Chem. Soc., Dalton Trans.*, 1993, Issue 1, pp. xxiii–xxviii.

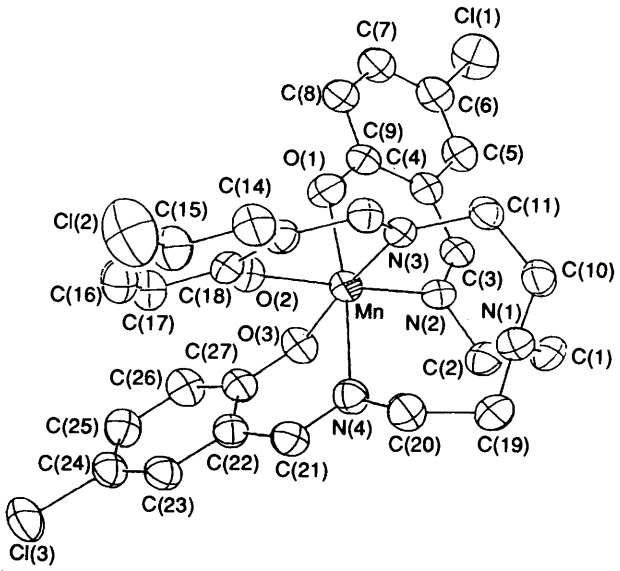

Fig. 1 ORTEP plot and labelling scheme for $[MnL^2]$ in $[MnL^2]$·MeOH. All atoms are represented by their 50% probability ellipsoids

Table 1 Selected bond lengths (Å) and angles (°) for $[MnL^2]$·MeOH with estimated standard deviations (e.s.d.s) in parentheses

Mn–O(1)	2.096(2)	Mn···N(1)	3.245(4)
Mn–O(2)	1.888(3)	Mn–N(2)	2.071(4)
Mn–O(3)	1.907(3)	Mn–N(3)	2.077(3)
O(1)–C(9)	1.299(5)	Mn–N(4)	2.370(3)
O(2)–C(18)	1.317(5)	O(3)–C(27)	1.328(5)
Cl(1)–C(6)	1.742(5)	O(4)–C(28)	1.246(17)
Cl(2)–C(15)	1.746(5)	Cl(3)–C(24)	1.746(5)
O(1)–Mn–O(2)	87.0(1)	O(2)–Mn–N(4)	83.5(1)
O(1)–Mn–O(3)	100.8(1)	O(3)–Mn–N(2)	84.1(1)
O(1)–Mn–N(2)	86.3(1)	O(3)–Mn–N(3)	170.9(1)
O(1)–Mn–N(3)	88.0(1)	O(3)–Mn–N(4)	82.3(1)
O(1)–Mn–N(4)	169.9(1)	N(2)–Mn–N(3)	98.5(1)
O(2)–Mn–O(3)	89.9(1)	N(2)–Mn–N(4)	103.5(1)
O(2)–Mn–N(2)	170.0(1)	N(3)–Mn–N(4)	88.6(1)
O(2)–Mn–N(3)	88.7(1)		

located *trans* to each other in $[MnL^2]$·MeOH are significantly elongated (by 0.1–0.2 Å) whilst the two other *trans* pairs are slightly compressed. In O_h symmetry the ground state of high-spin manganese(III) is $t_{2g}^3e_g^1$ which transforms to $e^2a^1e^1$ in C_3 symmetry. The degeneracy of the singly occupied antibonding orbital is thus conserved in C_3 symmetry which is therefore subject to Jahn–Teller distortion. The observed strict C_3 symmetry of the metal co-ordination sphere in $[MnL^2]$·$3H_2O$ is thus unexpected. The structure is not a dynamical average since the anisotropic thermal parameters are entirely normal[3,8] (see Fig. 2). Thus strong crystal forces have enforced a metastable axially symmetric geometry on the manganese(III) atom in $[MnL^2]$·$3H_2O$. The water–water and water–phenolate hydrogen bondings in the lattice[2,3] are believed to be important factors in stabilising the cubic lattice. When the water molecules are substituted by bulkier methanol molecules the extent of solvation decreases and a different lattice is formed in which the MnN_3O_3 sphere is free to distort. The result is an unsymmetrical structure (C_1 symmetry) significantly elongated along one direction. In the solution phase [MnL] type complexes are known to assume an unsymmetrical structure.[4]

In both $[MnL^2]$·$3H_2O$ and $[MnL^2]$·MeOH the MnN_3O_3 co-ordination sphere has facial geometry (Fig. 2). The two structures of $[MnL^2]$ represent a subtle type of isomerism sustained by crystalline forces. The results in Fig. 2 have certain similarities with the controversial phenomenon of bond-stretch

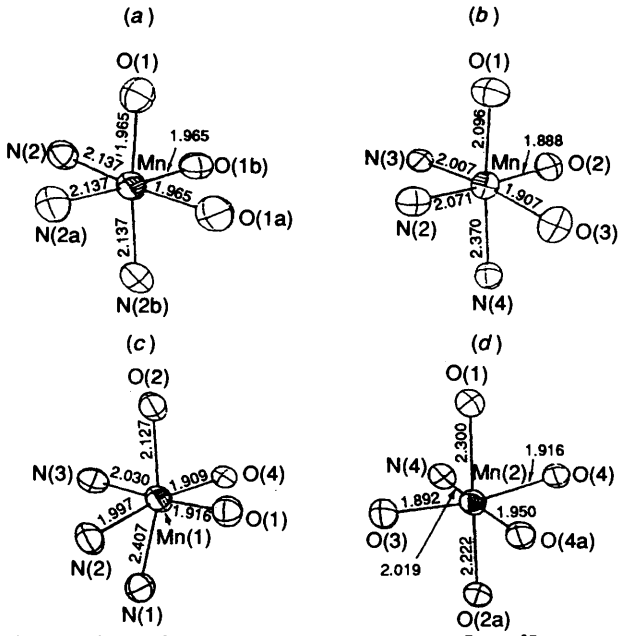

Fig. 2 Views of the co-ordination spheres in $[MnL^2]$·$3H_2O$ (*a*), $[MnL^2]$·MeOH (*b*) and $[Mn_4O_2L^1{}_2][PF_6]_2$·4MeCN (*c*) and (*d*). Bond lengths given in Å with e.s.d.s in the range 0.002–0.007 Å

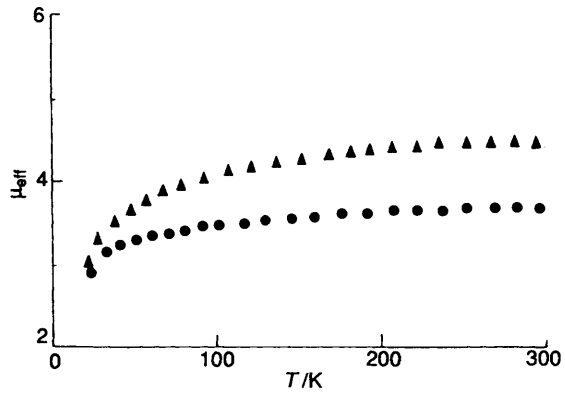

Fig. 3 Variable temperature magnetic moments (per metal atom) of $[Mn_4O_2L^1{}_2][PF_6]_2$ (●) and $[Mn_4O_2L^2{}_2][PF_6]_2$ (▲)

isomerism.[10] The difference is that the isomerism of $[MnL^2]$ is controlled by lattice forces and not by the existence of double minima along a bond-stretch coordinate.

Tetranuclear Complexes.—In [MnL] the full co-ordinating potential of the ligand is not utilised as the tripodal nitrogen is not co-ordinated at all and the phenolic oxygen atoms are potential bridging centres. The $N(CH_2CH_2^-)_3$ tripod is quite flexible and it seemed likely that some or all of the additional co-ordination could be activated by judicious choice of stoichiometry and reaction conditions.

We therefore examined the reactivity of [MnL] (L = L^1 or L^2) towards manganese(III) acetate dihydrate and it emerged that a very facile and nearly quantitative reaction occurs in alkaline acetonitrile ([MnL]: Mn^{3+} : OH^- 1:1:2) affording the green complex $[Mn_4O_2L_2]^{2+}$ isolated as the PF_6^- salt. The initially deposited solid contains solvent of crystallisation which is lost upon drying in air affording $[Mn_4O_2L_2][PF_6]_2$. The salts act as 1:2 electrolytes in solution and their absorption spectra in the visible region are qualitatively similar to those of [MnL], with bands near 600 and 1000 nm (Table 2).

The magnetic moments (300 K) of $[MnL^1]$·MeOH, $[MnL^2]$·MeOH and $[MnL^2]$·$3H_2O$ are 4.87, 4.82 and 4.85 respectively. The μ_{eff} values of $[Mn_4O_2L_2]^{2+}$ per metal atom are significantly smaller and these decrease progressively with tem-

Table 2 Analytical, electronic spectral and molar conductivity data

Compound	Analysis[a] (%) C	H	N	Mn	λ_{max}[b]/nm (ε/dm^3 mol^{-1} cm^{-1})	Λ[b]/Ω^{-1} cm^2 mol^{-1}
H_3L^1	70.70 (70.80)	6.50 (6.50)	12.20 (12.20)	—	—	—
H_3L^2	57.70 (57.70)	4.80 (4.80)	9.90 (10.00)	—	—	—
$[MnL^1]$·MeOH	62.00 (62.00)	5.70 (5.70)	10.30 (10.30)	10.10 (10.10)	320 (10 600), 380 (sh) (7900), 575 (sh) (550), 1000 (160)	—
$[MnL^2]$·MeOH	52.00 (52.10)	4.30 (4.30)	8.60 (8.70)	8.50 (8.50)	600 (600), 1100 (120)	—
$[Mn_4O_2L^1_2][PF_6]_2$	44.70 (44.70)	3.70 (3.70)	7.70 (7.70)	15.10 (15.10)	575 (sh) (1260), 980 (260)	280
$[Mn_4O_2L^2_2][PF_6]_2$	39.00 (39.10)	2.90 (2.90)	6.70 (6.70)	13.10 (13.20)	580 (1350), 1025 (270)	285

[a] Calculated values in parentheses. [b] In acetonitrile at 298 K.

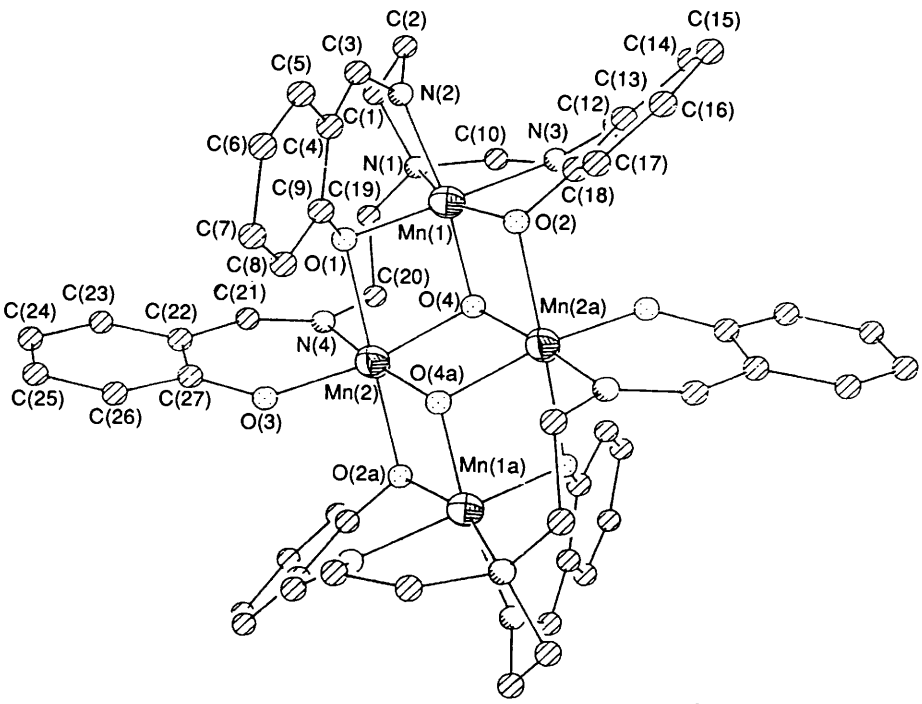

Fig. 4 A perspective view of the cation $[Mn_4O_2L^1_2]^{2+}$

perature (Fig. 3). In the range 300–20 K values lie in the ranges 3.73–2.86 and 4.51–3.05 for $[Mn_4O_2L^1_2]^{2+}$ and $[Mn_4O_2L^2_2]^{2+}$ respectively. The tetranuclear complexes are thus antiferromagnetic, the interaction being weaker in $[Mn_4O_2L^2_2]^{2+}$. This could be partly due to electron withdrawal by the chloro substituent from the exchange pathway.

The X-ray structure of the solvate $[Mn_4O_2L^1_2][PF_6]_2$·4MeCN has been determined. A view of the centrosymmetric tetranuclear cation is shown in Fig. 4 and selected bond parameters are listed in Table 3. Symmetry related atom pairs are identified as Mn(1), Mn(1a), N(1), N(1a) *etc.* The tripodal nitrogen [say N(1)] and two salicylaldimine arms incorporating the atom pairs N(2), O(1) and N(3), O(2) together with the oxide oxygen O(4) complete the six-co-ordination around Mn(1). The third salicylaldimine arm [N(4), O(3)] of the ligand is not bonded to Mn(1) but to Mn(2). The remaining four co-ordination positions of Mn(2) are occupied by bridging phenolato [O(1), O(2a)] and oxide [O(4), O(4a)] oxygen atoms. The distorted octahedral metal co-ordination spheres are thus of two types: facial N_3O_3 for Mn(1) [and Mn(1a) by symmetry] and NO_5 for Mn(2) [and Mn(2a)]. The co-ordination spheres are significantly elongated along the N(1)Mn(1)O(2) and O(1)Mn(2)O(2a) axes respectively. The spheres are compared with those $[MnL^2]$·$3H_2O$ and $[MnL^2]$·MeOH in Fig. 2.

The Mn(1) and Mn(2) atoms are bridged by oxide and phenolato oxygen atoms and by the third salicylaldimine arm noted above. The oxide ligands are μ_3-bridging and four phenolato oxygen atoms [O(1), O(1a), O(2) and O(2a)] are μ-bridging. The only non-bridging oxygens in $[Mn_4O_2L^1_2]^{2+}$ are the two symmetry related phenolato atoms O(3) and O(3a). In the $Mn_4(\mu_3\text{-}O)_2^{8+}$ core the four metal atoms lie on a plane and the oxide oxygen atoms are displaced from it by 0.858 Å in a mutually opposite direction.

The Mn(2)···Mn(2a) distance [2.906(3) Å] is the shortest metal–metal contact. Synthetic O- and/or N-co-ordinated Mn_4 complexes[11–15] having a Mn···Mn contact of < 3 Å are of interest in the bioinorganic chemistry of the water oxidation site of photosystem II.[16,17] The facile formation of $[Mn_4O_2L_2]^{2+}$ from [MnL] shows how a flexible polypeptide backbone having side chain O- and N-donors can organise oxidic Mn_4 ensembles.

The electroactivity of the tetranuclear complexes has been examined in acetonitrile solution using a platinum electrode. All potentials reported are referenced to saturated calomel electrode (SCE). The cyclic voltammogram of $[Mn_4O_2L^2_2]^{2+}$ is shown in Fig. 5 together with that of $[MnL^2]$. The $E_{\frac{1}{2}}$ values (Table 4) of the chloro-substituted L^2 complexes are systematically higher than those of the unsubstituted L^1 complexes as expected. The two values for [MnL] correspond to Mn^{III}–Mn^{II} and Mn^{IV}–Mn^{III} redox couples.[4,6]

In $[Mn_4O_2L_2]^{2+}$ two overlapping cyclic responses α and β (Fig. 5, Table 4) occur at potentials < 0.2 V. Coulometry at 200

Table 3 Selected bond lengths (Å) and angles (°) for $[Mn_4O_2L^1_2][PF_6]_2$·4MeCN with e.s.d.s in parentheses

Mn(1)–O(1)	1.916(5)	Mn(2)–O(1)	2.300(5)
Mn(1)–O(2)	2.127(5)	Mn(2)–O(2a)	2.222(5)
Mn(1)–O(4)	1.909(5)	Mn(2)–O(3)	1.892(5)
Mn(1)–N(1)	2.407(7)	Mn(2)–O(4)	1.916(5)
Mn(1)–N(2)	1.997(6)	Mn(2)–O(4a)	1.950(5)
Mn(1)–N(3)	2.030(6)	Mn(2)–N(4)	2.019(6)
Mn(1)···Mn(2)	3.000(3)	Mn(2)···Mn(1a)	3.042(3)
Mn(1)···Mn(1a)	5.297(3)	Mn(2)···Mn(2a)	2.906(3)
Mn(1)···Mn(2a)	3.042(3)	O(2)–C(18)	1.330(8)
O(1)–C(9)	1.343(9)	O(3)–C(27)	1.312(9)
P–F(1)	1.553(9)	P–F(4)	1.575(10)
P–F(2)	1.472(11)	P–F(5)	1.570(11)
P–F(3)	1.474(9)	P–F(6)	1.516(12)
O(1)–Mn(1)–O(2)	88.9(2)	O(1)–Mn(2)–O(2a)	177.4(2)
O(1)–Mn(1)–O(4)	87.7(2)	O(1)–Mn(2)–O(3)	89.8(2)
O(1)–Mn(1)–N(1)	109.1(2)	O(1)–Mn(2)–O(4)	77.3(2)
O(1)–Mn(1)–N(2)	86.4(2)	O(1)–Mn(2)–O(4a)	95.7(2)
O(1)–Mn(1)–N(3)	172.6(3)	O(1)–Mn(2)–N(4)	86.6(2)
O(2)–Mn(1)–O(4)	85.3(2)	O(2a)–Mn(2)–O(3)	90.1(2)
O(2)–Mn(1)–N(1)	162.0(2)	O(2a)–Mn(2)–O(4)	102.6(2)
O(2)–Mn(1)–N(2)	101.7(2)	O(2a)–Mn(2)–O(4a)	81.8(2)
O(2)–Mn(1)–N(3)	84.7(2)	O(2a)–Mn(2)–N(4)	95.9(2)
O(4)–Mn(1)–N(1)	96.6(2)	O(3)–Mn(2)–O(4)	166.7(2)
O(4)–Mn(1)–N(2)	170.7(2)	O(3)–Mn(2)–O(4a)	95.5(2)
O(4)–Mn(1)–N(3)	95.3(2)	O(3)–Mn(2)–N(4)	91.6(2)
N(1)–Mn(1)–N(2)	78.7(3)	O(4)–Mn(2)–O(4a)	82.5(2)
N(1)–Mn(1)–N(3)	77.4(3)	O(4)–Mn(2)–N(4)	91.1(2)
N(2)–Mn(1)–N(3)	91.4(3)	O(4a)–Mn(2)–N(4)	172.6(2)

mV below the cathodic peak potential of the couple α corresponds to a net transfer of two electrons (Table 4). Couples α and β are thus assigned to successive one-electron reductions (Mn^{III}–Mn^{II}) of two of the four metal centres. It is proposed that the centres are Mn(1) and Mn(1a) which as for the metal in [MnL] have facial MnN_3O_3 co-ordination spheres; significantly the $E_{\frac{1}{2}}$ values corresponding to α and β are not far removed from that of the Mn^{III}–Mn^{II} couple of [MnL]. The relatively small difference between the $E_{\frac{1}{2}}$ values of α and β is consistent with the proposed assignment since the Mn(1) and Mn(1a) atom pair have a relatively wide separation of 5.297(3) Å. Two overlapping oxidative responses γ and δ are observed above 0.4 V but the cathodic peaks are poorly defined. These electrochemical data are very different from those described elsewhere which were based on a poorly resolved voltammogram of $[Mn_4O_2L^1_2][ClO_4]_2$.[7]

In view of the very facile nature of the transformation of [MnL] to $[Mn_4O_2L_2]^{2+}$, it seemed logical that similar polynucleation may occur for other metal ions also. Preliminary results have been obtained for iron(III) systems. The complex $[FeL^2]$ (μ_{eff} = 5.88 at 298 K) is found[2] to react smoothly with iron(III) chloride in alkaline acetonitrile in the presence of PF_6^- affording a red-violet antiferromagnetic complex (μ_{eff} = 4.61 per iron atom at 298 K) of composition $[Fe_2OL^2]PF_6$. Its electrical conductivity (Λ = 280 Ω^{-1} cm^2 mol^{-1} in acetonitrile) is similar to that of $[Mn_4O_2L^2_2][PF_6]_2$ (Table 2). It is electroactive and affords two quasi-reversible Fe^{III}–Fe^{II} couples with $E_{\frac{1}{2}}$ = −0.57 and −0.22 V as opposed to $[FeL^2]$ which has only one such couple, $E_{\frac{1}{2}}$ = −0.62 V (Fig. 5). The indications are that the new complex may be an iron(III) congener of the tetranuclear manganese complex. Further studies are in progress.

Experimental

Materials.—The ligands H_3L^1 and H_3L^2 and the compound $[Mn(O_2CMe)_3]$·$2H_2O$ were prepared as reported previously.[2,18] Electrochemically pure acetonitrile, dimethylformamide and tetraethylammonium perchlorate were obtained as before.[19] All other chemicals and solvents were of analytical grade and used as obtained.

Table 4 Electrochemical data[a]

Compound	$E_{\frac{1}{2}}$/V
$[MnL^1]$·MeOH	−0.29, 0.54
$[MnL^2]$·MeOH	−0.13, 0.65
$[Mn_4O_2L^1_2][PF_6]_2$[b]	−0.20, 0.03, 0.87,[c] 1.01[c]
$[Mn_4O_2L^2_2][PF_6]_2$	−0.12, 0.14, 0.96,[c] 1.06[c]
$[FeL^2]$	−0.62
$[Fe_2OL^2]PF_6$[d]	−0.57, −0.22

[a] 298 K, $[NEt_4][ClO_4]$ (0.1 mol dm^{-3}) supporting electrolyte, platinum working electrode, SCE reference electrode, solvent for manganese and iron complexes acetonitrile and dimethylformamide respectively, solute concentration 10^{-3} mol dm^{-3}. [b] Constant potential (−0.45 V) coulometry gives Q/Q' = 0.99, where Q is the observed and Q' the calculated coulomb count for two-electron transfer. [c] Anodic peak potentials. [d] Empirical formula.

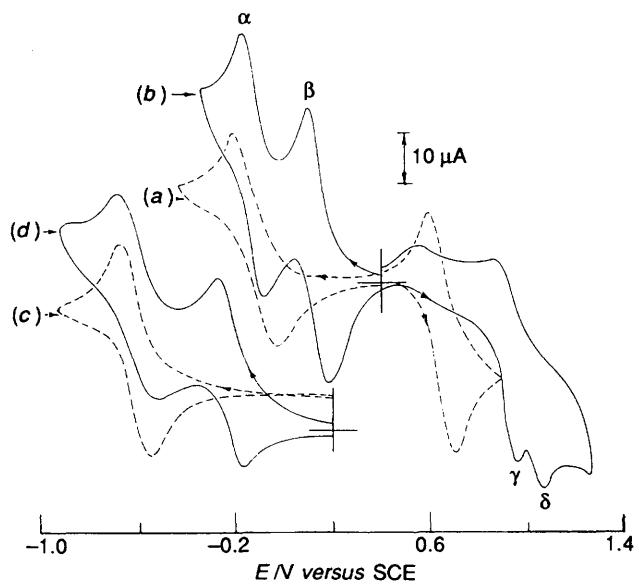

Fig. 5 Cyclic voltammograms (platinum electrode, 298 K) of $[MnL^2]$·MeOH (*a*) and $[Mn_4O_2L^2_2][PF_6]_2$ (*b*) (in acetonitrile) and $[FeL^2]$ (*c*) and $[Fe_2OL^2]PF_6$ (*d*) (in dimethylformamide) (10^{-3} mol dm^{-3}, 0.1 mol dm^{-3} $[NEt_4][ClO_4]$)

Physical Measurements.—Electronic spectra were recorded with a Hitachi 330 spectrophotometer. Magnetic susceptibilities were measured at 300 K using a PAR-155 vibrating-sample magnetometer fitted with a Walker Scientific L75FBAL magnet. Variable-temperature magnetic data were collected with a George Associates model 300 Lewis Coil force magnetometer. A Perkin-Elmer 240C elemental analyser was used to collect microanalytical data (C, H, N). Electrochemical measurements were performed at 298 K under pure, dry nitrogen with a PAR model 370-4 electrochemistry system as described elsewhere.[20] All potentials reported in this work are uncorrected for junction contribution. Solution (*ca.* 10^{-3} mol dm^{-3}) electrical conductivities were measured with a Philips PR 9500 bridge. Effective magnetic moments (μ_{eff}) per metal atom were calculated using $\mu_{eff} = 1.42\sqrt{\chi T}$, where χ is the corrected susceptibility of the tetranuclear complex and T is the absolute temperature.

Preparations.—*Mononuclear manganese*(III) *complexes.* To a methanolic solution (25 cm^3) of H_3L^2 (0.30 g, 0.53 mmol) was added $[Mn(O_2CMe)_3]$·$2H_2O$ (0.15 g, 0.56 mmol) followed by KOH (0.10 g, 1.78 mmol) and the mixture stirred with a

Table 5 Crystal data for $[MnL^2]$·MeOH and $[Mn_4O_2L^1{}_2][PF_6]_2$·4MeCN

Compound	$[MnL^2]$·MeOH	$[Mn_4O_2L^1{}_2][PF_6]_2$·4MeCN
Formula	$C_{28}H_{28}Cl_3MnN_4O_4$	$C_{62}H_{66}F_{12}Mn_4N_{12}O_8P_2$
M	645.8	1617.0
Crystal size/mm	0.14 × 0.29 × 0.42	0.16 × 0.30 × 0.32
Crystal system	Triclinic	Monoclinic
Space group	$P\bar{1}$ (no. 2)	$P2_1/n$ (no. 14)
a/Å	9.457(3)	14.019(7)
b/Å	11.731(3)	16.165(8)
c/Å	13.153(4)	15.995(7)
α/°	80.98(2)	—
β/°	78.76(3)	102.27(4)
γ/°	89.08(2)	—
U/Å^3	1413.4(7)	3542(3)
Z	2	2
D_c/g cm^{-3}	1.52	1.52
μ(Mo-Kα)/cm^{-1}	7.75	8.02
F(000)	664	1648
2θ range/°	2–50	2–50
Total number of reflections	5299	6943
Number of unique reflections	4968	6629
Number of observed reflections [$I > 3\sigma(I)$]	3476	3020
Transmission factor*	0.868	0.944
g in $w = 1/[\sigma^2(F) + gF^2]$	0.0001	0.0005
Number of refined parameters	361	451
R	4.61	6.04
R'	5.22	6.12
Goodness of fit	1.45	1.47
Maximum and mean Δ/σ	0.002, 0.001	0.002, 0.001
Data to parameter ratio	9.6:1	6.7:1
Maximum, minimum difference peaks/e Å^{-3}	0.67, −0.51	0.69, −0.51

* Maximum transmission factor is normalized to 1.0.

Table 6 Atomic coordinates (× 10^4) for $[MnL^2]$·MeOH with e.s.d.s in parentheses

Atom	x	y	z	Atom	x	y	z
Mn	3 949(1)	2 878(1)	8 745(1)	C(9)	3 213(4)	2 178(3)	11 177(3)
Cl(1)	4 165(2)	2 204(2)	14 431(1)	C(10)	7 473(4)	1 445(3)	8 121(3)
Cl(2)	1 684(2)	−1 012(1)	5 570(1)	C(11)	6 197(4)	980(3)	8 979(3)
Cl(3)	−504(1)	6 333(1)	5 752(1)	C(12)	4 383(4)	535(3)	8 109(3)
O(1)	2 901(3)	2 162(2)	10 260(2)	C(13)	3 201(4)	694(3)	7 558(3)
O(2)	2 336(3)	2 387(2)	8 269(2)	C(14)	3 005(5)	−121(3)	6 919(3)
O(3)	3 223(3)	4 409(2)	8 654(2)	C(15)	1 935(5)	13(4)	6 350(3)
O(4)	9 230(16)	1 447(13)	707(12)	C(16)	1 014(5)	941(4)	6 410(3)
N(1)	7 357(3)	2 672(3)	7 782(2)	C(17)	1 186(4)	1 744(3)	7 036(3)
N(2)	5 457(3)	3 530(3)	9 461(2)	C(18)	2 261(4)	1 632(3)	7 638(3)
N(3)	4 860(3)	1 276(2)	8 590(2)	C(19)	7 443(4)	3 077(4)	6 670(3)
N(4)	4 852(3)	3 482(3)	6 931(2)	C(20)	6 038(4)	2 923(4)	6 319(3)
C(1)	7 867(4)	3 457(4)	8 374(3)	C(21)	4 027(4)	4 113(3)	6 432(3)
C(2)	6 658(4)	4 248(3)	8 775(3)	C(22)	2 758(4)	4 719(3)	6 898(3)
C(3)	5 430(4)	3 439(3)	10 455(3)	C(23)	1 844(5)	5 197(3)	6 231(3)
C(4)	4 435(4)	2 790(3)	11 304(3)	C(24)	650(5)	5 801(3)	6 597(3)
C(5)	4 713(5)	2 791(3)	12 324(3)	C(25)	340(5)	5 973(3)	7 631(3)
C(6)	3 817(5)	2 192(4)	13 180(3)	C(26)	1 215(5)	5 500(3)	8 305(3)
C(7)	2 626(5)	1 584(4)	13 072(3)	C(27)	2 420(4)	4 846(3)	7 969(3)
C(8)	2 332(5)	1 579(3)	12 087(3)	C(28)	9 812(8)	2 355(10)	184(7)

magnetic stirrer for 0.5 h. The green solid which separated was redissolved in CH_2Cl_2 (15–20 cm^3) and the solvent evaporated slowly at room temperature. Green crystals of $[MnL^2]$·MeOH were formed over 2–3 d, yield 0.30 g (*ca.* 91%). Recrystallisation from wet acetonitrile deposited $[MnL^2]$·$3H_2O$. The complex $[MnL^1]$·MeOH was prepared similarly from H_3L^1.

Tetranuclear manganese(III) *complexes.* To a warm acetonitrile solution (25 cm^3) of $[MnL^1]$·MeOH (0.10 g, 0.18 mmol) was added $[Mn(O_2CMe)_3]$·$2H_2O$ (0.05 g, 0.18 mmol) and the mixture stirred with a magnetic stirrer. After 15 min methanolic KOH (0.02 g, 0.36 mmol) was added, followed by solid NH_4PF_6 (0.03 g, 0.18 mmol) and the mixture stirred for 3 h. Upon concentration and cooling (*ca.* 5 °C) green crystals of $[Mn_4O_2L^1{}_2][PF_6]_2$·4MeCN deposited. When dried in air, the crystals rapidly lost MeCN, leaving $[Mn_4O_2L^1{}_2][PF_6]_2$ as a powder. Yield of powder 0.125 g (*ca.* 93%). The complex $[Mn_4O_2L^2{}_2][PF_6]_2$ was synthesised similarly from $[MnL^2]$·MeOH.

Iron(III) *complexes.* The ligand H_3L^2 (0.15 g, 0.32 mmol) and $Fe^{II}[ClO_4]_2$·$6H_2O$ (0.10 g, 0.28 mmol) were mixed in acetonitrile (15 cm^3). Methanolic KOH (0.06 g, 1.06 mmol) was added and the solution was oxidised by air at room temperature for 2 h resulting in the deposition of the dark red complex $[FeL^2]$ (0.15 g, *ca.* 76%) (Found: C, 52.80; H, 4.00; Fe, 8.90; N, 9.00. Calc. for $C_{27}H_{24}Cl_3FeN_4O_3$: C, 52.80; H, 3.90; Fe, 9.00; N, 9.10%).

To a warm acetonitrile solution (25 cm^3) of $[FeL^2]$ (0.20 g, 0.32 mmol) was added solid $FeCl_3$ (0.05 g, 0.30 mmol) and the

Table 7 Atomic coordinates ($\times 10^4$) for $[Mn_4O_2L^1{}_2][PF_6]_2 \cdot 4MeCN$ with e.s.d.s in parentheses

Atom	x	y	z	Atom	x	y	z
Mn(1)	1756(1)	563(1)	726(1)	C(7)	−619(6)	2125(7)	2195(6)
Mn(2)	−164(1)	748(1)	−513(1)	C(8)	−386(6)	1820(6)	1456(6)
O(1)	769(3)	1395(3)	663(3)	C(9)	568(6)	1671(5)	1399(5)
O(2)	1104(3)	−97(3)	1610(3)	C(10)	3426(9)	188(9)	−205(8)
O(3)	−1074(3)	1627(3)	−633(3)	C(11)	3294(9)	−476(7)	261(7)
O(4)	864(3)	−32(3)	−133(3)	C(12)	3034(6)	−770(5)	1655(6)
N(1)	2859(4)	965(4)	−167(4)	C(13)	2562(6)	−755(5)	2364(5)
N(2)	2639(4)	1342(4)	1497(4)	C(14)	3081(7)	−1126(5)	3150(7)
N(3)	2778(5)	−344(4)	950(4)	C(15)	2652(10)	−1186(7)	3833(6)
N(4)	652(4)	1356(4)	−1213(4)	C(16)	1706(9)	−904(8)	3772(6)
N(5)	4532(7)	336(8)	7882(6)	C(17)	1193(6)	−556(6)	3034(5)
N(6)	7602(9)	1466(8)	3954(7)	C(18)	1603(5)	−451(5)	2319(5)
P	6210(2)	2789(3)	974(2)	C(19)	2465(6)	1276(6)	−1048(6)
F(1)	6908(7)	3065(9)	1816(7)	C(20)	1474(6)	937(5)	−1493(5)
F(2)	5416(7)	3236(9)	1249(9)	C(21)	507(6)	2116(5)	−1459(5)
F(3)	5631(8)	2500(7)	146(5)	C(22)	−226(6)	2667(5)	−1259(5)
F(4)	7148(6)	2302(7)	859(6)	C(23)	−175(7)	3503(6)	−1499(6)
F(5)	6541(7)	3525(7)	462(8)	C(24)	−823(8)	4073(6)	−1314(7)
F(6)	5861(7)	2040(8)	1395(7)	C(25)	−1535(7)	3817(6)	−883(7)
C(1)	3477(7)	1619(7)	353(7)	C(26)	−1616(6)	2994(6)	−640(5)
C(2)	3618(6)	1469(6)	1297(6)	C(27)	−961(5)	2403(5)	−832(5)
C(3)	2319(6)	1786(5)	2045(6)	C(28)	4208(9)	494(7)	7225(8)
C(4)	1315(6)	1840(5)	2119(5)	C(29)	3824(11)	692(9)	6342(10)
C(5)	1078(7)	2144(6)	2856(6)	C(30)	8171(14)	1087(9)	3820(9)
C(6)	128(8)	2278(7)	2924(6)	C(31)	8993(20)	549(13)	3812(18)

mixture stirred with a magnetic stirrer. After 0.5 h, methanolic KOH (10 cm^3, 0.035 g, 0.62 mmol) was added followed by solid NH_4PF_6 (0.05 g, 0.30 mmol). The mixture was kept warm and stirred for 6 h. Upon evaporation at room temperature a red-violet solid deposited which was recrystallised from acetonitrile affording a complex of composition $[Fe_2OL^2]PF_6$ in pure form (0.20 g, *ca.* 74%) (Found: C, 39.10; H, 3.00; Fe, 13.30; N, 6.70. Calc. for $C_{27}H_{24}Cl_3F_6Fe_2N_4O_4P$: C, 39.00; H, 2.90; Fe, 13.40; N, 6.70%).

X-Ray Structure Determinations.—Single crystals of $[MnL^2]\cdot MeOH$ were grown by slow evaporation from a 1:1 dichloromethane–methanol solution. Crystals of $[Mn_4O_2L^1{}_2][PF_6]_2\cdot 4MeCN$ grown from acetonitrile on cooling were immediately coated with an epoxy resin to prevent solvent loss. Cell dimensions were determined by the least-squares refinement of automatically centred reflections {25 for $[MnL^2]\cdot MeOH$, 30 for $[Mn_4O_2L^1{}_2][PF_6]_2\cdot 4MeCN$, in the 2θ range 15–30°}. Data were collected at 296 K on a Nicolet R3m/V diffractometer with graphite monochromated Mo-Kα (λ = 0.710 73 Å) radiation in the ω–2θ scan mode. Two check reflections measured after every 98 reflections showed no significant variations in either case. Lorentz and polarization corrections and a semi-empirical absorption correction [21] were applied.

Both the structures were solved by direct methods and were refined by full-matrix least-squares procedures. All the non-hydrogen atoms were refined anisotropically and hydrogen atoms were included at calculated positions with isotropic thermal parameters (0.08 $Å^2$). Crystal data and other details are collected in Table 5. Final fractional atomic coordinates are given in Tables 6 and 7. Computations were carried out on a Micro VAXII computer using the SHELXTL-PLUS program system [22] and crystal structure plots were drawn using ORTEP. [23]

Additional material available from the Cambridge Crystallographic Data Centre comprises H-atom coordinates, thermal parameters and remaining bond lengths and angles.

Acknowledgements

We thank the Department of Science and Technology, New Delhi, for financial support. Crystallography was performed at the National Single Crystal Diffractometer Facility established by the same Department. The Council of Scientific and Industrial Research provided a fellowship to one of us (P. C.). We also thank Professor C. N. R. Rao, Indian Institute of Science, Bangalore for the variable temperature magnetic data. Affiliation to the Jawaharlal Nehru Centre for Advanced Scientific Research, Bangalore, India, is also acknowledged.

References

1 J. A. Broomhead and D. J. Robinson, *Aust. J. Chem.*, 1968, **21**, 1365.
2 D. F. Cook, D. Cummins and E. D. McKenzie, *J. Chem. Soc., Dalton Trans.*, 1976, 1369.
3 N. W. Alcock, D. F. Cook, E. D. McKenzie and J. M. Worthington, *Inorg. Chim. Acta*, 1980, **38**, 107.
4 K. Ramesh, D. Bhuniya and R. N. Mukherjee, *J. Chem. Soc., Dalton Trans.*, 1991, 2917.
5 K. Ramesh and R. N. Mukherjee, *J. Chem. Soc., Dalton Trans.*, 1991, 3259.
6 S. K. Chandra and A. Chakravorty, *Inorg. Chem.*, 1991, **30**, 3795.
7 C. Gedye, C. Harding, V. McKee and J. Nelson, *J. Chem. Soc., Chem. Commun.*, 1992, 392.
8 S. K. Chandra and A. Chakravorty, unpublished work.
9 S. K. Chandra, Ph.D. Thesis, Jadavpur University, Calcutta, 1992.
10 Y. Jean, A. Lledos, J. K. Burdett and R. Hoffman, *J. Am. Chem. Soc.*, 1988, **110**, 4506; J. Song and M. B. Hall, *Inorg. Chem.*, 1991, **30**, 4433; V. C. Gibson and M. McPartlin, *J. Chem. Soc., Dalton Trans.*, 1992, 947 and refs. therein.
11 J. B. Vincent, C. Christmas, H.-R. Chang, Q. Li, P. D. W. Boyd, J. C. Huffman, D. N. Hendrickson and G. Christou, *J. Am. Chem. Soc.*, 1989, **111**, 2086; J. B. Vincent, C. Christmas, J. C. Huffman, G. Christou, H.-R. Chang and D. N. Hendrickson, *J. Chem. Soc., Chem. Commun.*, 1987, 236; C. Christmas, J. B. Vincent, J. C. Huffman, G. Christou, H.-R. Chang and D. N. Hendrickson, *J. Chem. Soc., Chem. Commun.*, 1987, 1303.
12 R. J. Kulawiec, R. H. Crabtree, G. W. Brudvig and G. K. Schulte, *Inorg. Chem.*, 1988, **27**, 1309.
13 J. S. Bashkin, H.-R. Chang, W. E. Streib, J. C. Huffman, D. N. Hendrickson and G. Christou, *J. Am. Chem. Soc.*, 1987, **109**, 6502; Q. Li, J. B. Vincent, E. Libby, H.-R. Chang, J. C. Huffman, P. D. W. Boyd, G. Christou and D. N. Hendrickson, *Angew. Chem., Int. Ed. Engl.*, 1988, **27**, 1731.
14 M. K. Chan and W. H. Armstrong, *J. Am. Chem. Soc.*, 1990, **112**, 4985; M. K. Chan and W. H. Armstrong, *J. Am. Chem. Soc.*, 1991, **113**, 5055.
15 E. Libby, J. K. McCusker, E. A. Schmitt, K. Folting, D. N. Hendrickson and G. Christou, *Inorg. Chem.*, 1991, **30**, 3486; S. Wang,

K. Folting, W. E. Streib, E. A. Schmitt, J. K. McCusker, D. N. Hendrickson and G. Christou, *Angew. Chem., Int. Ed. Engl.*, 1991, **30**, 305; S. Wang, J. C. Huffman, K. Folting, W. E. Streib, E. B. Lobkovsky and G. Christou, *Angew. Chem., Int. Ed. Engl.*, 1991, **30**, 1672; M. Mikuriya, Y. Yamato and T. Tokii, *Chem. Lett.*, 1991, 1429; M. Suzuki, Y. Hayashi, K. Munezawa, M. Suenaga, H. Senda and A. Uehara, *Chem. Lett.*, 1991, 1929.

16 G. W. Brudvig, H. H. Thorp and R. H. Crabtree, *Acc. Chem. Res.*, 1991, **24**, 311; J. Amesz, *Biochim. Biophys. Acta*, 1983, **726**, 1; G. C. Dismukes, *Photochem. Photobiol.*, 1986, **43**, 99; G. N. George, R. C. Prince and S. P. Cramer, *Science*, 1989, **243**, 789; V. K. Yachandra, R. D. Guiles, A. E. McDermott, J. L. Cole, R. D. Britt, S. L. Dexheimer, K. Sauer and M. P. Klein, *Biochemistry*, 1987, **26**, 5974.

17 J. B. Vincent and G. Christou, *Adv. Inorg. Chem.*, 1989, **33**, 197; V. L. Pecoraro, *Photochem. Photobiol.*, 1988, **48**, 249; K. Wieghardt, *Angew Chem., Int. Ed. Engl.*, 1989, **28**, 1153.

18 *Handbook of Preparative Inorganic Chemistry*, ed. G. Brauer, Academic Press, New York, 1965, vol. 2, p. 1469.

19 D. Datta, P. K. Mascharak and A. Chakravorty, *Inorg. Chem.*, 1981, **20**, 1673.

20 S. K. Chandra, P. Basu, D. Ray, S. Pal and A. Chakravorty, *Inorg. Chem.*, 1990, **29**, 2423.

21 A. C. T. North, D. C. Phillips and F. S. Mathews, *Acta Crystallogr., Sect. A*, 1968, **24**, 351.

22 G. M. Sheldrick, SHELXTL-PLUS 88, Structure Determination Software Programs, Nicolet Instrument Corporation, Madison, WI, 1988.

23 C. K. Johnson, ORTEP, Report ORNL-5138, Oak Ridge National Laboratory, Oak Ridge, TN, 1976.

Received 24*th November* 1992; *Paper* 2/06304B